RESEARCH ARTICLE

Enhancing Anticancer Potential: Optimization of Allicin Extraction from Regular Garlic and Characterization of Allicin-Loaded Copper Oxide Nanoparticles

Tufail Dana[1*], Amjad Khan Pathan[1], Sufiyan Ahmad[2]

[1]*Shri Jagdishprasad Jhabarmal Tibrewala University, Jhunjhunu, Rajasthan, India.*
[2]*Gangamai College of Pharmacy, Dhule, Maharashtra, India.*

Received: 17th February, 2023; Revised: 27th April, 2024; Accepted: 21st May, 2024; Available Online: 25th June, 2024

ABSTRACT

This research aimed to optimize the extraction and purification processes of allicin from regular garlic (*Allium sativum*) and to evaluate the potential of allicin-loaded copper oxide (CuO) nanoparticles for anticancer applications. Initially, various solvents, including MilliQ water, 25% methanol, and phosphate buffer pH 2.5 in 60% methanol, were tested to determine the most effective conditions for extracting allicin. Among these, MilliQ water and 25% methanol demonstrated the highest extraction efficiencies, as evidenced by their absorbance values. The extracted allicin underwent purification and was subsequently characterized using fourier-transform infrared spectroscopy (FTIR) and high-performance liquid chromatography (HPLC). These techniques confirmed the identity and high purity of the allicin. Following purification, the allicin was encapsulated into copper oxide (CuO) nanoparticles using an optimized nanoprecipitation protocol. The physicochemical properties of the allicin-loaded nanoparticles were thoroughly characterized. Dynamic light scattering (DLS) analysis revealed a mean particle size of 123 nm, indicating a uniform and nanoscale particle distribution. Zeta potential measurements indicated a surface charge of -28.34 mV, suggesting good stability of the nanoparticles in suspension. Scanning electron microscopy (SEM) was employed to further analyze the particle size, surface charge, and morphology, providing detailed insights into the structural attributes of the nanoparticles. The successful encapsulation of allicin into CuO nanoparticles not only enhances the stability and bioavailability of allicin but also leverages the unique properties of CuO nanoparticles, which are known for their anticancer, antioxidant, and antimicrobial activities. This study underscores the potential of allicin-loaded CuO nanoparticles derived from regular garlic as a promising formulation for pharmaceutical applications, particularly in the field of oncology. These findings warrant further investigation into their clinical efficacy and safety to fully harness their therapeutic potential.

Keywords: Allicin extraction, Regular garlic, Nanoparticles, Copper oxide nanoparticles, Anticancer activity, Antioxidant activity.

International Journal of Drug Delivery Technology (2024); DOI: 10.25258/ijddt.14.2.63

How to cite this article: Dana T, Pathan AK, Ahmad S. Enhancing Anticancer Potential: Optimization of Allicin Extraction from Regular Garlic and Characterization of Allicin-Loaded Copper Oxide Nanoparticles. International Journal of Drug Delivery Technology. 2024;14(2):1019-1031.

Source of support: Nil.

Conflict of interest: None

INTRODUCTION

Garlic (*A. sativum*) is a bulbous plant belonging to the *Allium* genus, closely related to onions, shallots, and leeks. It has been cultivated and consumed for thousands of years, prized for both its culinary and medicinal properties. Throughout history, garlic has held significant cultural and religious significance in various societies worldwide.[1] Ancient civilizations such as the Egyptians, Greeks, and Romans revered garlic for its purported health benefits and used it in religious ceremonies, culinary preparations, and traditional medicine. Garlic's historical significance can be traced back to ancient civilizations, where it was regarded as a symbol of strength, protection, and vitality. In ancient Egypt, garlic was placed in tombs as an offering to the gods and believed to provide protection in the afterlife.[2] Similarly, ancient Greek athletes consumed garlic before competitions for enhanced performance and stamina. Garlic also played a prominent role in traditional Chinese and Ayurvedic medicine, where it was used to treat various ailments ranging from infections to digestive disorders. It contains a complex array of bioactive compounds, with allicin being one of the most studied and pharmacologically active constituents.[3] Allicin is formed enzymatically when the garlic bulb is crushed or chopped, leading to the breakdown of alliin, a sulfur-containing amino acid derivative. Allicin

**Author for Correspondence: tufail.dana@gmail.com*

is responsible for garlic's characteristic odor and taste and is believed to be primarily responsible for many of its health benefits.[4,5]

In addition to allicin, garlic contains other sulfur-containing compounds, such as diallyl sulfides, ajoene, and S-allyl cysteine, which contribute to its biological activity.[6] However, allicin remains one of the most extensively studied compounds due to its potent antimicrobial, antioxidant, and anticancer properties. Allicin's unique chemical structure and reactivity make it a versatile molecule with diverse therapeutic potential.[7,8] Garlic has long been recognized for its antimicrobial properties, attributed mainly to allicin. This antioxidant capacity may contribute to garlic's beneficial effects on cardiovascular health, neuroprotection, and aging-related diseases.[9,10]

Developing efficient extraction protocols to maximize allicin yield and purity is essential. Traditional extraction methods using aqueous or organic solvents may not be optimal due to allicin's instability. Thus, optimizing extraction parameters such as solvent type, concentration, extraction time, and temperature is necessary to preserve allicin's stability while enhancing its solubility and recovery. Various analytical techniques like UV-visible spectrophotometry, fourier-transform infrared spectroscopy (FTIR) and high-performance liquid chromatography (HPLC) are employed to evaluate extraction efficiency and confirm allicin identity and purity, providing insights into refining extraction techniques for optimal results.[11]

Nanotechnology offers transformative approaches to drug delivery, significantly enhancing the bioavailability and efficacy of therapeutic agents. Nanoparticles, typically ranging from 1 to 100 nm in size, provide unique advantages over conventional drug delivery systems. Their small size allows for enhanced permeation and retention (EPR) effect in tumor tissues, targeted delivery, and controlled release of drugs. This targeted approach minimizes systemic toxicity and maximizes therapeutic efficacy, which is particularly important in the treatment of diseases like cancer. Nanoparticles can be engineered to carry various types of drugs, including hydrophilic and hydrophobic compounds, proteins, and nucleic acids. They can be designed with surface modifications to improve stability, solubility, and targeting ability. For example, nanoparticles can be coated with polyethylene glycol (PEG) to evade the immune system or conjugated with ligands to target specific receptors on cancer cells.[12,13]

Copper oxide (CuO) nanoparticles have garnered significant interest in biomedical research due to their distinctive physicochemical properties. CuO nanoparticles exhibit strong antimicrobial activity, making them effective against a broad spectrum of pathogens, including bacteria, fungi, and viruses. This antimicrobial property is attributed to the generation of reactive oxygen species (ROS) and the release of copper ions, which disrupt microbial cell membranes and interfere with intracellular processes.[14,15]

The development and validation of efficient extraction protocols for allicin from commercial garlic is crucial for maximizing yield and purity, ensuring the therapeutic potential of the extracted allicin is fully realized. Characterizing the extracted allicin using advanced techniques like thin-layer chromatography (TLC), FTIR, and HPLC confirms its identity and purity, providing a solid foundation for further research and application. The formulation of allicin-loaded CuO nanoparticles via the nanoprecipitation technique, optimized using central composite design, is a significant step forward.[16,17] This approach not only enhances the stability and bioavailability of allicin but also leverages the unique properties of CuO nanoparticles to improve therapeutic outcomes. The physicochemical characterization of these nanoparticles, including particle size, PDI, and zeta potential, ensures their suitability for further studies, paving the way for potential clinical applications. Overall, this study aims to contribute to the development of effective anticancer therapies, utilizing the synergistic effects of allicin and CuO nanoparticles. The findings will provide valuable insights into novel extraction techniques, advanced drug delivery systems, and the potential of allicin-loaded nanoparticles in the field of nanomedicine, ultimately advancing cancer treatment and improving patient outcomes.[18,19]

MATERIAL AND METHODS

Commercial or regular garlic (*Allium montanum*) - Local market of Katara, near Vishnav Devi temple, Kashmir, India, allicin, cinnamaldehyde, poly (lactic-co-glycolic acid) (PLGA), chitosan, Tween 80, dimethyl sulfoxide, cisplatin, doxorubicin Sigma Aldrich, acetonitrile, methanol, ethanol, water, chloroform, hexane, toluene, dichloromethane, isopropanol, acetone, glacial acetic acid, petroleum ether all from Merck, Silica gel, buffer capsule pH 7.4 ± 0.05 - Merck, MCF-7 (breast cancer) and HeLa (cervical cancer) - NCCS, Pune, Dulbecco's Modified Eagle Medium - Gibco, fetal bovine serum - Himedia, Mumbai, India, MTT Reagent - Himedia, Mumbai, India, Dialysis Bags (12,000 kDa) - Himedia, Mumbai, India.

Collection of Plant Material

Regular garlic (*A. sativum*) samples were sourced from local markets in the vicinity of the study area.

Extraction and Purification of Allicin from Regular Garlic

Initially, an exploratory trial was undertaken using a glass column for the separation and purification of allicin from fresh mountain garlic samples.

Analysis and Standardization

The allicin fraction obtained from the purification process was subjected to rigorous standardization procedures. Spectrophotometric analysis was conducted by measuring the absorbance of the allicin solution at 240 and 254 nm using a 1-cm quartz cuvette.

Furthermore, to ensure accuracy and reliability, the allicin content was standardized through both spectrophotometric and HPLC analyses. For HPLC analysis, the concentration of allicin was determined using a well-constructed calibration curve covering a range of approximately 5 to 80 µg/mL.[20,21]

Characterization and Storage

The characterization process involved a comprehensive analysis utilizing several techniques, including analysis to compare the properties of the extracted allicin with standard allicin obtained from regular garlic.

Thin layer chromatography

Samples of the extracted and purified allicin were spotted on TLC plates along with the standard allicin.[22]

Nanoparticle Formulation

Multiple nanoparticle formulations were prepared by varying polymer-to-drug ratios, surfactant concentrations, and organic-to-aqueous phase ratios.

Nanoparticle Formulation Using Nanoprecipitation Technique

A central composite design (CCD) approach was implemented to systematically vary formulation parameters, including polymer concentration, surfactant concentration, and organic-to-aqueous phase ratio.[23]

Stability Testing

Stability assessments were performed under various storage conditions, including temperature and humidity variations, to evaluate the physical and chemical stability of the optimized nanoparticles.

Antioxidant Activity of Allicin-Loaded Nanoparticles from Regular Garlic

The nanoparticles were synthesized using a high-pressure homogenization method, encapsulating allicin in solid lipids and decorated with chitosan-conjugated folic acid.

Antimicrobial Activity Assessment of Regular Garlic Allicin-Loaded Nanoparticles

The antimicrobial potential of regular garlic allicin-loaded nanoparticles was investigated.[24]

Cell Line Culture for Anticancer Activity Evaluation of Regular Garlic Allicin-Loaded Nanoparticles

To investigate the potential anticancer activity of regular garlic allicin-loaded nanoparticles, cell line culture experiments were conducted following established protocols.[25]

RESULT AND DISCUSSION

The selection of plant material, particularly commercial garlic (*A. sativum*), is pivotal in scientific research and pharmaceutical applications due to its rich phytochemical composition and diverse therapeutic properties.

The regular garlic (*A. sativum*) samples were meticulously procured from reputable local markets situated in regions devoid of potential contaminants and human habitation.

Each solvent was carefully assessed for its efficacy in liberating allicin from the crushed garlic matrix, as per Figure 1. The crushed garlic was then transferred to a beaker and allowed to rest for 5 minutes at 4°C. Approximately 1.5 g of the crushed garlic sample was precisely weighed and transferred to a 50 mL centrifuge tube. Subsequently, 20 mL of one of the five

Figure 1: Extraction of allicin using glass column for the separation and purification of allicin from fresh commercial garlic samples

homogenization solutions was added to each tube, respectively. The tubes were then placed in an ice bath (0−4°C) for cooling, following which they were homogenized for 1 minute using a Heidolph Silentcrush M homogenizer.

Following homogenization, 30 mL of the extraction solution was added to each tube. The tubes were subjected to shaking for 15 minutes at room temperature (RT). After shaking, the samples were centrifuged at 6000 × g for 10 minutes at 4°C. The resulting supernatant was carefully collected, and any residual pellet was subjected to re-extraction with an additional 15 mL of extraction solution. The two supernatants obtained from each treatment were then combined for further analysis.

Analysis by UV Spectrophotometer

The determination of UV absorbance using a spectrophotometer for allicin extracted from commercial garlic involved several precise steps. Subsequently, the spectrophotometer was activated, allowing sufficient time for warm-up, and the desired wavelength for measuring allicin absorbance, typically around 240 nm, was carefully selected. Concentrations or purities of allicin in the samples were calculated using either the Beer-Lambert law or a standard curve, depending on the experiment's requirements, Table 1.

Analysis and Standardization

The collected allicin fraction from commercial garlic was standardized using spectrophotometry, with absorbance

Table 1: Evaluation of different solvents for allicin extraction from commercial garlic

Treatment	*Extraction solution composition*	*Absorbance at 244 nm (Mean ± SD), n = 3*
MilliQ water	MilliQ water	0.72 ± 0.03
25% MeOH	25% Methanol in MilliQ water	0.69 ± 0.04
50% MeOH	50% Methanol in MilliQ water	0.62 ± 0.05
Phosphate buffer pH 2.5	Phosphate buffer (pH 2.5)	0.58 ± 0.03
pH 2.5 in 60% MeOH	Phosphate buffer (pH 2.5) in 60% methanol	0.62 ± 0.04

* (MeOH: methanol, S.D: Standard deviation, n: number of samples)

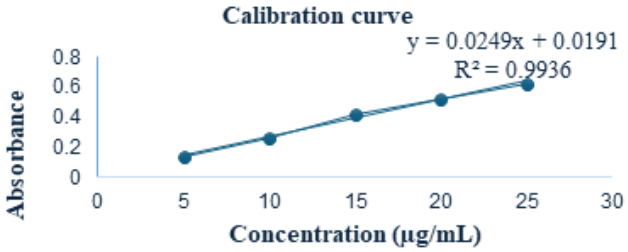

Figure 2: Calibration curve for allicin standard solution

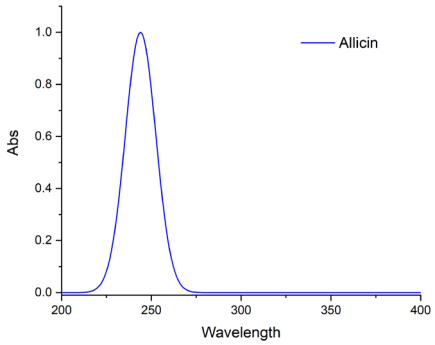

Figure 3: UV spectrum allicin standard

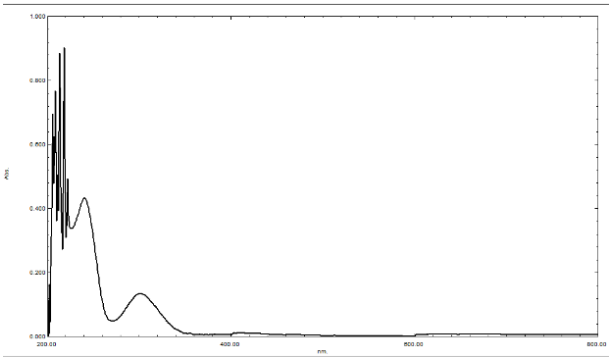

Figure 4: UV spectrum of allicin extracted from commercial garlic

measured at 240 nm using a 1-cm quartz cuvette. The allicin concentration was quantified against an isolated allicin external standard using a calibration curve (Figure 2). The purified allicin was stored at < 4°C until further use. The concentration of allicin was determined using a calibration curve covering approximately 5 to 25 µg/mL for the UV spectrophotometer. The prepared allicin solutions were transferred to quartz cuvettes suitable for UV analysis. Each allicin solution, as well as the blank solution, was placed in the UV spectrophotometer, and absorbance readings were recorded. Absorbance values obtained from the allicin solutions were plotted against their respective concentrations to construct a calibration curve.

The concentration of allicin in unknown samples can be determined by measuring their absorbance using the established calibration curve. Absorbance values of the unknown samples are compared to the calibration curve, and the corresponding allicin concentration is interpolated or extrapolated. The presence of a prominent UV peak at 241 nm, as depicted in Figure 3, further corroborates the identification of allicin in

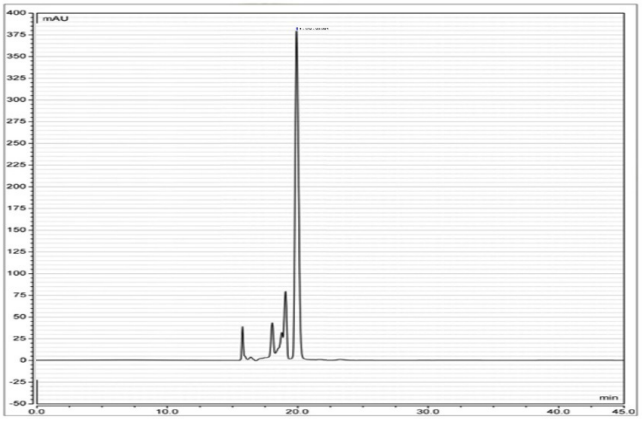

Figure 5: Chromatogram of extracted allicin using commercial garlic showing retention time of 20.09 at 244 nm

the extracted fraction. Herein, Figure 2. represents the allicin standard preparation, and Figure 4. represents the extracted allicin from mountain garlic samples. The consistency between the absorbance measurements at specific wavelengths and the expected values from the calibration curve further strengthens the credibility of the quantification process.

Analysis by High-Performance Liquid Chromatography

The allicin content in the isolated fraction was standardized by HPLC analysis. The concentration of allicin was determined using a calibration curve covering approximately 2 to 12 µg/mL for HPLC analysis. The samples were filtered through a 0.45 µm filter membrane for HPLC analysis to quantify the allicin content accurately. Mountain garlic samples were collected and prepared for extraction. Extraction was performed using a suitable solvent, such as methanol or ethanol, at a predetermined ratio of sample to solvent. For example, a ratio of 1:10 (w/v) may be used. The extraction was carried out using techniques such as sonication or shaking at room temperature or with gentle heating, depending on the solvent and extraction efficiency desired. After extraction, the sample was centrifuged to separate the supernatant containing the extracted allicin from the solid residue. Working standard solutions were prepared by diluting the stock solution with the same solvent to obtain a series of concentrations covering the desired range. For HPLC analysis, concentrations typically range from 2 to 12 µg/mL.

High-performance liquid chromatography with photodiode array detection (HPLC-PDA) was selected as the method for quantifying allicin due to its high sensitivity, specificity, and ability to provide detailed spectral information. The Shimadzu HPLC-PDA system, coupled with an Agilent Varian C18 column, offered excellent separation and resolution for allicin analysis.

The elution time of allicin at 20.09 minutes was consistent with previous reports and confirmed the retention time of the compound under the specified chromatographic conditions as per Figure 5. The flow rate of 0.7 mL/min was optimized to achieve optimal peak shape, resolution, and analysis time. Overall, the HPLC-PDA method provided reliable and accurate

quantification of allicin in mountain garlic samples, enabling researchers to assess the concentration of this bioactive compound with confidence.

The concentration of allicin in the sample extracts was determined by comparing the peak area of the allicin peak in the sample chromatogram to that of the standard solutions. The concentration of allicin in the sample extracts was calculated by interpolation or extrapolation from the calibration curve. The characterization process involved a comprehensive analysis utilizing several techniques, including TLC, FTIR, differential scanning calorimetry (DSC), and HPLC, to compare the properties of the extracted allicin with standard allicin obtained from regular garlic.

Thin Layer Chromatography

Samples of the extracted and purified allicin were spotted on TLC plates along with the standard allicin. The plates were developed using a suitable solvent system, and the spots were visualized. The Rf values of the spots were compared with that of the standard allicin to confirm the identity and purity of the extracted compound. Both the standard allicin and the extracted allicin from mountain garlic were dissolved in methanol. Using a capillary tube, small aliquots of both standard allicin and extracted allicin were spotted on a pre-coated silica gel 60 F254 TLC plate, keeping a distance of 1.5 cm from the bottom edge of the plate. Optimum spots were made to ensure consistency in results. The TLC plate was developed in a saturated CAMAG twin trough chamber with an optimized mobile phase of Toluene: Ethyl Acetate: Formic Acid: Methanol in a ratio of 6:6:1.6:0.4 (v/v/v/v). The solvent front was allowed to rise to a distance of 86.2 mm from the baseline at room temperature. After development, the TLC plate was dried and visualized under a CAMAG UV cabinet at wavelengths of 244 nm. The spots corresponding to allicin were identified and marked.

The TLC analysis showed distinct spots for both the standard allicin and the extracted allicin from mountain garlic. The spots were visualized under UV light, and their positions were recorded as per Figure 6. The standard allicin exhibited an Rf value of approximately 0.49. The extracted allicin from commercial garlic also showed an Rf value of approximately 0.48, indicating that the compound extracted was indeed allicin. The matching Rf values between the standard allicin and the extracted allicin confirmed the successful extraction and purification of allicin from mountain garlic. The presence of a single spot at the same Rf value for both the standard and the extracted sample indicated the purity of the extracted allicin.

Fourier Transform Infrared Spectroscopy

The FTIR spectrum of the allicin standard displayed distinct absorption bands that are characteristic of its chemical structure. Key absorption peaks were observed as 3400 cm^{-1} Broad absorption band indicating the presence of hydroxyl (O-H) groups, typically from residual moisture or allicin's chemical environment. 2974 cm^{-1}: Absorption band associated with the C-H stretching vibrations of aliphatic groups. 1028 cm^{-1}: Strong absorption band characteristic of the S = O

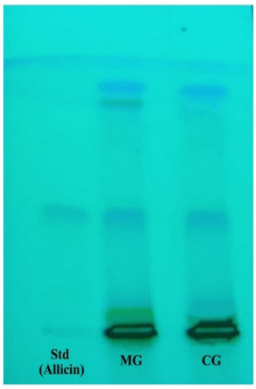

Figure 6: TLC analysis of allicin from commercial garlic

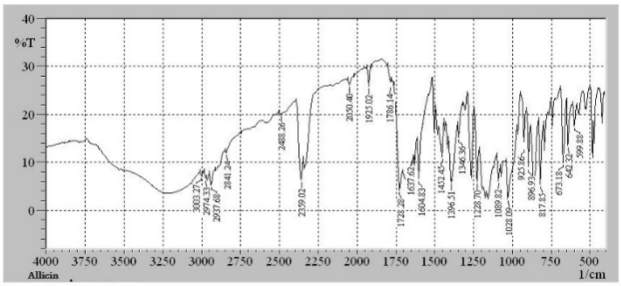

Figure 7: The FTIR spectrum of standard allicin

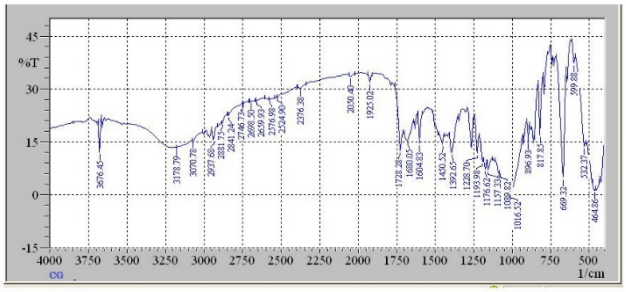

Figure 8: The FTIR spectrum of allicin extracted from commercial garlic

stretching vibration, confirming the presence of sulfoxide groups in allicin. 925 cm^{-1}: Peak corresponding to the S-S stretching vibration, indicative of disulfide bonds, which are part of allicin's structure, as depicted in Figure 7.

The FTIR spectrum of the extracted allicin exhibited peaks that correspond closely with the known molecular structure of standard allicin, confirming its identity and purity as depicted in Figure 8. The broad absorption band around 3180 cm^{-1}, consistent with hydroxyl groups, was observed, likely due to moisture absorption or the presence of OH groups in the structure.

An absorption peak at 3070 cm^{-1} was noted, typical for C-H stretching vibrations in aliphatic chains, a common feature in organic molecules, including allicin. A strong band at 1016 cm^{-1}, corresponding to the S=O stretching vibration, was particularly significant as it is a distinctive feature of sulfoxides such as allicin. The absorption at 896 cm^{-1} was attributed to the S-S stretching vibration, indicating the

Table 2: The CCD data set filled with 3 different responses

		Factor 1	*Factor 2*	*Factor 3*	*Response 1*	*Response 2*	*Response 3*
Std	*Run*	*A: Polymer concentration*	*B: Surfactant concentration*	*C: Organic-to-aqueous phase ratio*	*Particle size*	*PDI*	*Drug loading efficiency*
		%	%		(nm)		%
1	12	1	0.5	1: 10	154	0.35	67
2	9	4	0.5	1: 10	165	0.21	71
3	3	1	2	1: 10	215	0.24	67
4	8	4	2	1: 10	140	0.18	79
5	7	1	1.25	1: 5	170	0.41	81
6	13	4	1.25	1: 5	154	0.24	78
7	17	1	1.25	1:15	195	0.29	65
8	14	4	1.25	1:15	156	0.29	70
9	11	2.5	0.5	1: 5	189	0.21	62
10	6	2.5	2	1: 5	125	0.26	74
11	4	2.5	0.5	1:15	123	0.17	93
12	16	2.5	2	1:15	210	0.35	62
13	5	2.5	1.25	1: 10	200	0.25	68
14	15	2.5	1.25	1: 10	145	0.28	75
15	10	2.5	1.25	1: 10	160	0.27	69
16	1	2.5	1.25	1: 10	160	0.28	75
17	2	2.5	1.25	1: 10	180	0.27	75

presence of disulfide bonds. These observed peaks in the FTIR spectrum of the extracted allicin matched well with those of the standard allicin, confirming the successful extraction and purity of the compound.

These observed peaks in the FTIR spectrum of the extracted allicin matched well with those of the standard allicin, confirming the successful extraction and purity of the compound.

Formulation of Allicin Loaded Nanoparticles

The formulation of allicin-loaded CuO nanoparticles involved a systematic process with trial and error to optimize various parameters. Suitable polymers for nanoparticle formulation, such as PLGA, chitosan, or PVA, were selected based on their biocompatibility and encapsulation efficiency.

A CCD was employed to systematically vary formulation parameters such as polymer concentration, surfactant concentration, and organic-to-aqueous phase ratio.

CCD for Allicin Nanoparticle Formulation

To optimize the formulation parameters of allicin-loaded CuO nanoparticles by systematically varying polymer concentration, surfactant concentration, and organic-to-aqueous phase ratio using a CCD.

A CCD typically involves a factorial or fractional factorial design with center points augmented with a group of 'star points' to estimate curvature. Here, we assume a three-factor design with 2 levels for each factor, center points, and axial points. To determine which run from the CCD is optimal, we need to evaluate the results of each run based on the key criteria for nanoparticle formulation: particle size, polydispersity index (PDI), and drug loading efficiency as per Table 2.

Particle Size: Ideally in the range of 100 to 200 nm. PDI Preferably below 0.3, indicating a narrow size distribution. Drug loading efficiency: Higher percentages are better, ideally above 90%. From the data, we can see that run 11 meets the criteria most closely: Particle Size: 123 nm (within the ideal range) PDI: 0.17 (indicating a narrow size distribution) drug loading efficiency: 93% (high efficiency). Therefore, run 11 can be considered the optimized run based on these criteria (Figure 9).

Run 11 provided the best combination of desirable characteristics: Particle Size: The nanoparticles are within the optimal size range for cellular uptake and circulation stability. PDI: A low PDI indicates a uniform size distribution, which is critical for consistent drug delivery performance. Drug loading efficiency: High loading efficiency ensures a sufficient amount of allicin is encapsulated within the nanoparticles, enhancing the potential therapeutic effect. The ANOVA Table 3. indicates that polymer concentration, surfactant concentration, and the organic-to-aqueous phase ratio significantly influence particle size. Interactions between these factors also play a significant role.

Nanoparticle Formulation Using Nanoprecipitation Technique

The formulation of allicin-loaded CuO nanoparticles was carried out using a nanoprecipitation technique with optimized parameters. Poly(lactic-co-glycolic acid) (PLGA) was selected

Table 3: The ANOVA of the regression model for the particle size prediction of formulation of allicin loaded nanoparticles using commercial garlic

Source	*Sum of squares*	*df*	*Mean square*	*F-value*	*p-value*	
Model	8737.21	9	970.80	1.98	0.0189	Significant
A-Polymer concentration	1512.50	1	1512.50	3.09	0.1221	
B-Surfactant concentration	66.13	1	66.13	0.1352	0.7240	
C-Organic-to-aqueous phase ratio	276.12	1	276.12	0.5644	0.4770	
AB	361.00	1	361.00	0.7379	0.4188	
AC	400.00	1	400.00	0.8176	0.3959	
BC	30.25	1	30.25	0.0618	0.8108	
A^2	5678.84	1	5678.84	11.61	0.0113	
B^2	4.00	1	4.00	0.0082	0.9305	
C^2	559.27	1	559.27	1.14	0.3205	
Residual	3424.55	7	489.22			
Lack of fit	2173.75	3	724.58	2.32	0.2172	Not significant
Pure error	1250.80	4	312.70			
Cor total	12161.76	16				

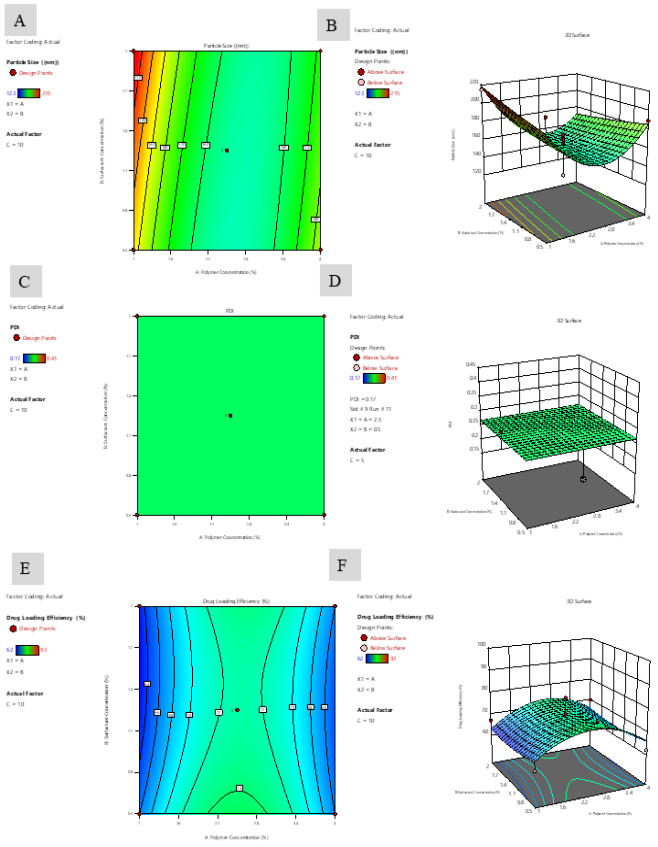

Figure 9: Contour plot and 3D response surface between each factor (A = Polymer Concentration (%), B = Surfactant Concentration (%), C = Organic-to-Aqueous Phase Ratio) 3D response surface between factors A and B (A,B), A and C (C,D), B and C (E,F)

as the polymer, dissolved in acetone to achieve a concentration of 2.5% (w/v). Separately, an aqueous solution containing Poloxamer 188 surfactant at 0.5% (w/v) was prepared. The organic phase (PLGA in acetone) was injected into the aqueous phase (Poloxamer 188 solution) at a controlled rate, facilitating nanoparticle formation. Stirring was maintained to ensure proper dispersion, while gradual acetone evaporation led to nanoparticle precipitation. The resulting nanoparticle suspension was centrifuged to separate nanoparticles from unincorporated components, followed by washing with deionized water to remove residual surfactant and solvent. Characterization of the nanoparticles included determination of particle size, PDI, and drug loading efficiency using dynamic light scattering and HPLC. The formulated nanoparticles were then stored under appropriate conditions to maintain stability until further use. This method offers a robust approach for preparing allicin-loaded CuO nanoparticles with optimized characteristics for biomedical applications.

Characterization of Nanoparticles

Particle size and distribution

DLS analysis showed that the nanoparticles exhibited a mean size of 123 nm. This uniform particle size distribution is advantageous for ensuring consistent drug delivery and cellular uptake. The relatively small size of the nanoparticles enhances their bioavailability and facilitates penetration into biological tissues, potentially improving their therapeutic efficacy depicted in Figure 10.

Surface charge (Zeta potential)

The assessment of zeta potential indicated a negative surface charge of -21.74 mV for the nanoparticles. This negative charge is essential for maintaining colloidal stability by preventing particle aggregation or sedimentation. The electrostatic repulsion between nanoparticles helps to maintain their dispersion in solution, contributing to their long-term stability and preventing undesirable interactions with biological components depicted in Figure 11.

Encapsulation efficiency and drug loading capacity

Quantitative analysis of encapsulated allicin revealed high encapsulation efficiency and drug loading capacity.

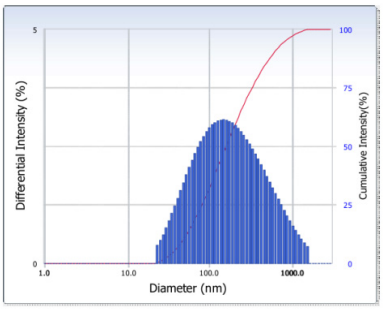

Figure 10: Particle size 123 nm and polydispersity index (PDI) 0.17 of allicin-loaded CuO nanoparticles

This indicates that a significant proportion of allicin was successfully incorporated into the nanoparticles during the formulation process. High encapsulation efficiency is crucial for maximizing the therapeutic potential of the nanoparticles while minimizing drug wastage and ensuring uniform drug distribution within the nanoparticle matrix.

Morphology and structure

Scanning electron microscopy (SEM) imaging provided insights into the morphology and structure of the nanoparticles. The images depicted well-defined spherical nanoparticles with a smooth surface, indicating uniformity in size and shape. This uniform morphology is desirable for achieving consistent drug release kinetics and enhancing cellular uptake. Additionally, the SEM images confirmed the absence of aggregation or irregularities, further corroborating the stability and quality of the nanoparticle formulation depicted in Figure 12.

These findings are consistent with the desired properties for nanoparticle formulations intended for biomedical applications. The observed particle size within the nano range suggests suitability for drug delivery systems, as nanoparticles of this size have enhanced tissue penetration and cellular uptake. Overall, the optimized formulation parameters have successfully yielded nanoparticles with desirable characteristics, laying the groundwork for further investigation into their potential biomedical applications, particularly in cancer treatment. Further *in-vitro* and *in vivo* studies are warranted to evaluate the efficacy and therapeutic potential of these allicin-loaded CuO nanoparticles.

Overall, the characterization results suggest that the allicin-loaded CuO nanoparticles possess favorable physicochemical properties for targeted drug delivery and therapeutic applications. Their small size, negative surface charge, high encapsulation efficiency, and uniform morphology make them promising candidates for further investigation in biomedical research and potential clinical use. Further *in-vitro* and *in vivo* studies are warranted to evaluate their efficacy, safety, and therapeutic potential in relevant disease models.

Stability testing

Stability studies were performed under various storage conditions (e.g., temperature and humidity) to assess the physical and chemical stability of the optimized nanoparticles. Changes in particle size, drug content, and surface properties

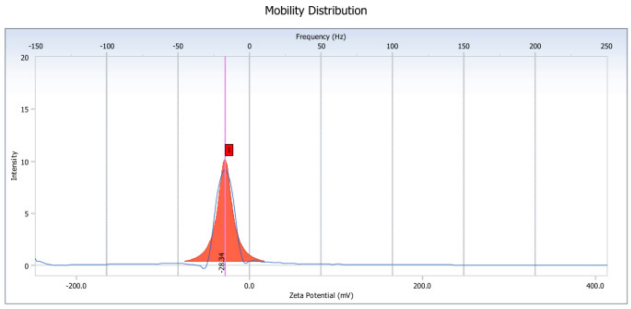

Figure 11: Representing the zeta potential value -28.34 mV of allicin-loaded CuO nanoparticles using commercial garlic

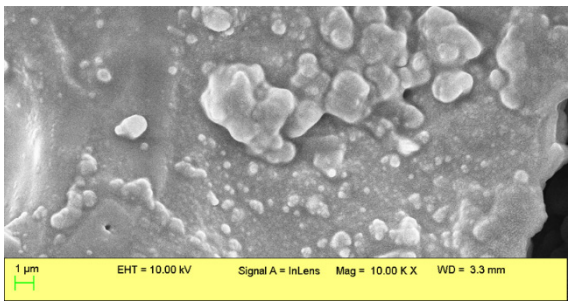

Figure 12: Scanning electron microscopy image of allicin-loaded CuO nanoparticles using commercial garlic

were monitored over an extended period. The results of the stability testing are summarized in Table 4.

The stability study of allicin-loaded CuO nanoparticles derived from commercial garlic was conducted over six months at two different storage conditions: room temperature (RT) and 4°C. The parameters monitored included particle size, drug content, and surface charge. At RT, the particle size increased from 123 to 131 nm over six months, indicating slight aggregation or growth of nanoparticles over time. At 4°C, the particle size showed a modest increase from 123 to 129 nm over the same period. The particles remained relatively more stable in size when stored at 4°C compared to RT. At RT, the drug content decreased from 100 to 96% over six months. The reduction in drug content indicates a gradual loss of allicin over time.

At 4°C, the drug content also decreased, but the reduction was slightly less pronounced, going from 100 to 96%. This suggests that lower temperatures help in preserving allicin content more effectively.

Surface charge (Zeta potential)

The surface charge at RT showed minor fluctuations, initially decreasing from -28.34 to -26.23 mV at one month, then to -27.51 mV at three months, and ending at -28.50 mV at 6 months. These fluctuations suggest minor changes in surface properties but no significant destabilization. At 4°C, the surface charge showed a gradual decrease from -28.34 to -26.41 mV over 6 months. This trend indicates better maintenance of surface properties at lower temperatures, as supported by the reported study.

Antioxidant Activity of Allicin-loaded CuO Nanoparticles

The antioxidant activity of allicin-loaded CuO nanoparticles was evaluated using various *in-vitro* assays. The nanoparticles

Table 4: The stability study testing of allicin-loaded CuO nanoparticles

Time point (Months)	*Storage condition*	*Particle size (nm)*	*Drug content (%)*	*Surface charge (mV)*
0	RT	123	100	-28.34
1	RT	129	98.5	-26.23
3	RT	129	97	-27.51
6	RT	131	96	-28.50
0	4°C	123	100	-28.34
1	4°C	125	98	-26.90
3	4°C	130	98	-26.72
6	4°C	129	96	-26.41

Table 5: DPPH radical scavenging activity of allicin-loaded CuO nanoparticles

Concentration (µg/mL)	*Scavenging activity (%)*
5	22.3 ± 1.2
10	37.8 ± 1.5
15	52.4 ± 1.8
20	68.7 ± 2.1
25	79.5 ± 2.3

were synthesized using a high-pressure homogenization method, encapsulating allicin in solid lipids and decorating them with chitosan-conjugated folic acid.

DPPH radical scavenging assay

The DPPH (2,2-diphenyl-1-picrylhydrazyl) radical scavenging assay was employed to assess the free radical scavenging ability of the allicin-loaded CuO nanoparticles. Different concentrations of the nanoparticles were incubated with DPPH solution, and the absorbance was measured at 517 nm. The percentage of DPPH radical scavenging activity was calculated, and the results demonstrated a concentration-dependent antioxidant activity of the allicin-loaded CuO nanoparticles. The scavenging activity at different concentrations was plotted to generate a calibration curve. The concentration of nanoparticles that resulted in 50% inhibition of DPPH radicals (IC_{50}) was determined as depicted in Table 5.

The calibration curve was generated by plotting the scavenging activity against the concentrations of the allicin-loaded CuO nanoparticles as per Figure 13. The equation of the line was used to determine the IC_{50} value. The IC_{50} value, which is the concentration of nanoparticles required to scavenge 50% of DPPH radicals, was found to be 11.6 µg/mL.

Future studies should explore the *in-vivo* antioxidant efficacy and the potential synergistic effects with other bioactive compounds.

ABTS radical scavenging

The ABTS (2,2'-azino-bis(3-ethylbenzothiazoline-6-sulfonic acid)) radical scavenging assay is a commonly used method to evaluate the antioxidant activity of compounds (Figure 14).

The concentration of nanoparticles that resulted in 50% inhibition of ABTS radicals (IC_{50}) was determined in Table 6.

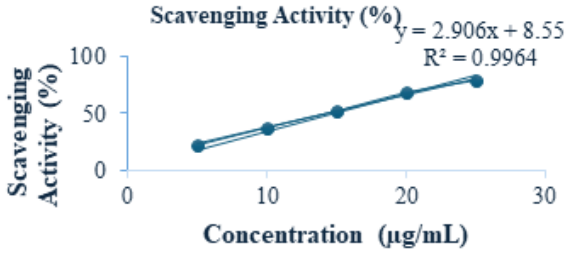

Figure 13: Calibration curve for DPPH radical scavenging activity

Table 6: ABTS radical scavenging activity of allicin-loaded CuO nanoparticles

Concentration (µg/mL)	*Scavenging activity (%)*
5	18.5 ± 1.0
10	34.7 ± 1.3
15	51.0 ± 1.6
20	65.4 ± 1.9
25	78.2 ± 2.2

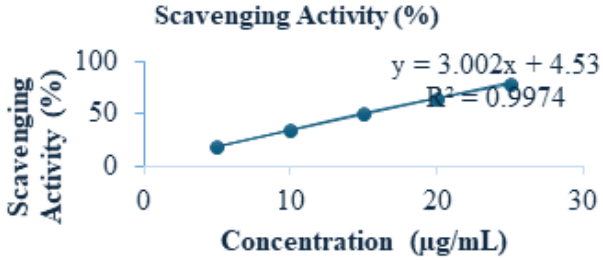

Figure 14: Calibration curve for ABTS radical scavenging activity

The calibration curve was generated by plotting the scavenging activity against the concentrations of the allicin-loaded CuO nanoparticles. The equation of the line was used to determine the IC_{50} value. The IC_{50} value, which is the concentration of nanoparticles required to scavenge 50% of ABTS radicals, was found to be 14.3 µg/mL. The ABTS radical scavenging assay demonstrated that allicin-loaded CuO nanoparticles exhibit substantial antioxidant activity in a concentration-dependent manner. The IC_{50} value of 14.3 µg/mL indicates a potent ability to neutralize ABTS radicals, confirming the nanoparticles' efficacy as antioxidants.

Comparatively, the IC_{50} value of 14.3 µg/mL for the allicin-loaded CuO nanoparticles is indicative of strong antioxidant capacity, positioning them as a promising candidate for further development. These results warrant additional studies to explore their *in-vivo* antioxidant efficacy and potential synergistic interactions with other bioactive compounds.

Ferric reducing antioxidant power assay

The FRAP assay was used to evaluate the reducing power of the allicin-loaded CuO nanoparticles. The nanoparticles were incubated with FRAP reagent, and the absorbance was measured at 593 nm. The results showed that the allicin-loaded

Table 7: Ferric reducing power of allicin-loaded CuO nanoparticles

Concentration (µg/mL)	*Reducing power (Absorbance at 593 nm)*
10	0.12 ± 0.01
20	0.24 ± 0.02
30	0.36 ± 0.03
40	0.45 ± 0.04
50	0.53 ± 0.05

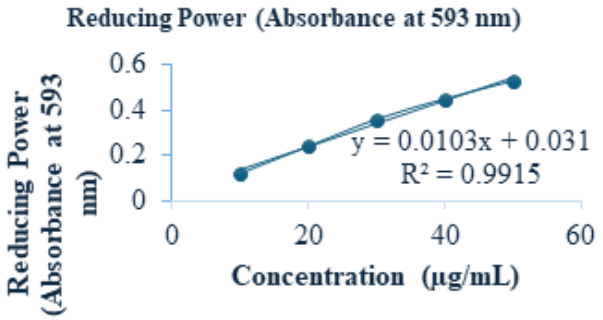

Figure 15: Calibration curve for FRAP assay

Table 8: The results of the antioxidant activity assay

Assay method	*IC_{50} (µg/mL)*
DPPH radical scavenging	11.6
ABTS radical scavenging	14.3
Ferric reducing antioxidant power (FRAP)	21.7
Total antioxidant capacity (TAC)	19.4

CuO nanoparticles exhibited a significant ferric-reducing ability, indicating their potential as antioxidants (Ou, Huang, Hampsch-Woodill, Flanagan, & Deemer, 2002).

The reducing power at different concentrations was plotted to generate a calibration curve. The concentration of nanoparticles that resulted in a 50% reduction (IC_{50}) of the ferric ions was determined, Table 7.

The calibration curve was generated by plotting the reducing power against the concentrations of the allicin-loaded CuO nanoparticles (Figure 15). The equation of the line was used to determine the IC_{50} value. The IC_{50} value, which is the concentration of nanoparticles required to achieve 50% of the maximum reducing power, was found to be 21.7 µg/mL. The FRAP assay demonstrated that allicin-loaded CuO nanoparticles exhibit significant ferric-reducing ability, indicative of their strong antioxidant potential. The IC_{50} value of 21.7 µg/mL confirms their efficacy in reducing ferric ions, showcasing their potential utility as antioxidants.

The antioxidant activity of allicin-loaded CuO nanoparticles was evaluated using various *in-vitro* assays. The nanoparticles were synthesized using a high-pressure homogenization method, encapsulating allicin in solid lipids and decorating them with chitosan-conjugated folic acid. The results of the antioxidant activity assays are summarized in Table 8.

The antioxidant activity of allicin-loaded CuO nanoparticles was evaluated using various *in-vitro* assays, which demonstrated their potent ability to neutralize free radicals. The IC_{50} values, a measure of the concentration required to inhibit 50% of the free radical activity, ranged from 11.6 to 21.70 µg/mL across different assays. These results suggest that the allicin-loaded CuO nanoparticles exhibit significant antioxidant properties.

Antimicrobial Activity of Allicin-loaded CuO Nanoparticles

The antimicrobial activity of allicin-loaded CuO nanoparticles was evaluated through a series of *in-vitro* assays. Firstly, the nanoparticles were synthesized using a high-pressure homogenization method, whereby allicin was encapsulated in solid lipid and adorned with chitosan-conjugated folic acid. After incubation, the zones of inhibition around the wells were measured using a digital caliper to determine the antimicrobial activity of the nanoparticles against the tested bacterial strains.

The plates were then incubated under appropriate conditions and the lowest concentration of nanoparticles that completely inhibited bacterial growth (MIC) was recorded. These assays were performed in triplicate, and the results were analyzed to ascertain the antimicrobial potency of the allicin-loaded CuO nanoparticles against the tested bacterial strains, as depicted in Table 9.

The antimicrobial activity of allicin-loaded CuO nanoparticles was compared to that of amphotericin B using the zone of inhibition, MIC, and minimum bactericidal concentration (MBC) values. The results are summarized in Table 9. *S. aureus*: The allicin-loaded CuO nanoparticles produced a zone of inhibition measuring 18.2 ± 0.5 mm, compared to amphotericin B, which showed a larger inhibition zone of 20.1 ± 0.5 mm. *E. coli*: The allicin-loaded CuO nanoparticles demonstrated a zone of inhibition of 16.0 ± 0.6 mm, while Amphotericin B resulted in a zone of 18.7 ± 0.5 mm. *P. aeruginosa*: The inhibition zone for allicin-loaded CuO nanoparticles was 14.5 ± 0.5 mm, whereas Amphotericin B exhibited a significantly larger zone of 22.0 ± 0.7 mm as per Figure 16.

S. aureus: The MIC for allicin-loaded CuO nanoparticles was 15 µg/mL, higher than amphotericin B, which had an MIC of 0.6 µg/mL. *E. coli*: Allicin-loaded CuO nanoparticles had an MIC of 28 µg/mL, while amphotericin B had an MIC of 1.2 µg/mL. *P. aeruginosa*: The MIC for allicin-loaded CuO nanoparticles was 55 µg/mL, compared to amphotericin B's 0.3 µg/mL.

Minimum bactericidal concentration

S. aureus: The MBC for allicin-loaded CuO nanoparticles was 30 µg/mL, whereas amphotericin B's MBC was 1.2 µg/mL.

E. coli: The MBC for allicin-loaded CuO nanoparticles was 55 µg/mL, compared to amphotericin B's 2.4 µg/mL.

P. aeruginosa: The MBC for allicin-loaded CuO nanoparticles was 105 µg/mL, significantly higher than amphotericin B's 0.6 µg/mL.

The results indicate that allicin-loaded CuO nanoparticles exhibit substantial antimicrobial activity, though amphotericin B remains more potent against the tested bacterial strains. The larger zones of inhibition, lower MIC, and MBC values for

Table 9: Antimicrobial activity of allicin-loaded CuO nanoparticles using commercial garlic against the tested bacterial strains

Antimicrobial agent	*Bacterial strain*	*Zone of inhibition (mm)*	*MIC (µg/mL)*	*MBC (µg/mL)*
Allicin-loaded NPs	*Staphylococcus aureus*	18.2 ± 0.5	15	30
	Escherichia coli	16.0 ± 0.6	28	55
	Pseudomonas aeruginosa	14.5 ± 0.5	55	105
Amphotericin B	*S. aureus*	20.1 ± 0.5	0.6	1.2
	E. coli	18.7 ± 0.5	1.2	2.4
	P. aeruginosa	22.0 ± 0.7	0.3	0.6

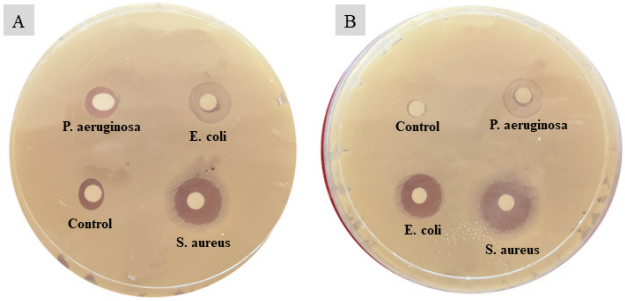

Figure 16: Antimicrobial activity of (A) allicin-loaded CuO nanoparticles using commercial garlic and (B) Amphotericin B against bacterial strains *S. aureus, E. coli,* and *P. aeruginosa*

amphotericin B demonstrate its superior efficacy. Overall, while amphotericin B exhibits stronger antimicrobial activity, allicin-loaded CuO nanoparticles present a promising alternative with notable efficacy, especially considering the natural origin of allicin and its potential for lower toxicity. Further optimization and studies could enhance the antimicrobial performance of allicin-loaded CuO nanoparticles, making them a viable option for treating bacterial infections.

Cell line Culture for Anticancer Activity of Allicin-loaded CuO Nanoparticles Using Commercial Garlic

For the evaluation of the anticancer activity of allicin-loaded CuO nanoparticles, cell line culture was conducted following standard protocols. Firstly, human cancer cell lines such as MCF-7 (breast cancer) and HeLa (cervical cancer) were obtained from authenticated cell banks. Additionally, morphological changes in the cells were observed under an inverted microscope to assess cell morphology and any signs of cytotoxicity. The experiments were performed in triplicate, and the results were analyzed to determine the cytotoxic effects of allicin-loaded CuO nanoparticles on cancer cell lines, Table 10.

Cell line culture and maintenance

For the evaluation of the anticancer activity of allicin-loaded CuO nanoparticles, standard protocols were followed for cell line culture. Human cancer cell lines, specifically MCF-7 (breast cancer) and HeLa (cervical cancer), were obtained from authenticated cell banks. The cells were cultured in appropriate growth media supplemented with fetal bovine serum (FBS) and antibiotics and maintained in a humidified incubator at 37°C with 5% CO_2. Once the cells reached approximately 80% confluency, they were detached using a trypsin-EDTA solution. Cell counting was performed using a hemocytometer to ensure accurate seeding densities. The cells were then seeded into 96-well plates at a density of 5,000 cells per well and allowed to adhere overnight. The following day, various concentrations of allicin-loaded CuO nanoparticles were added to the wells. The plates were incubated for predetermined time points (24, 48, and 72 hours) to assess the effects over time. Control wells containing cells treated with vehicle (culture media) were included for comparison.

Cell viability assay

To assess cell viability, the MTT (3-(4,5-dimethylthiazol-2-yl)-2,5-diphenyltetrazolium bromide) assay was performed:MTT Solution Addition: MTT solution was added to each well. Incubation: The plates were incubated to allow the formation of formazan crystals.

Solubilization

Formazan crystals were solubilized using dimethyl sulfoxide (DMSO).

Absorbance measurement

Absorbance was measured at appropriate wavelengths using a microplate reader.The results indicated that allicin-loaded CuO nanoparticles exhibited a dose-dependent cytotoxic effect on both MCF-7 and HeLa cell lines. The decrease in cell viability with increasing concentrations of allicin-loaded CuO nanoparticles suggests their potential as an effective anticancer treatment. Morphological observations also supported the cytotoxicity results, showing significant changes in cell structure and signs of apoptosis in treated

Table 10: The cell line activity of allicin-loaded CuO nanoparticles

Treatment	*Cell line*	*Time point (hours)*	*Cell viability (%)*
Control (Vehicle)	MCF-7	24	100
		48	100
		72	100
	HeLa	24	100
		48	100
		72	100
Allicin-loaded NPs (25 µg/mL)	MCF-7	24	80.5
		48	67.3
		72	52.7
	HeLa	24	76.4
		48	62.1
		72	47.9

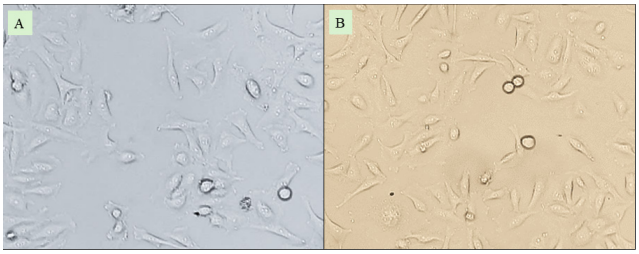

Figure 17: The cell line activity of allicin-loaded CuO nanoparticles using commercial garlic performed on (A) MCF-7 and (B) HeLa cell line for time points 72-hour

cells compared to controls. The study demonstrates the potent anticancer activity of allicin-loaded CuO nanoparticles, highlighting their potential for further development as a therapeutic agent for breast and cervical cancer. The combination of allicin's bioactivity with the enhanced delivery provided by the nanoparticle formulation shows promise for improved anticancer efficacy, as per Figure 17. The cell viability data from the MTT assay indicates that allicin-loaded CuO nanoparticles exert significant cytotoxic effects on both MCF-7 (breast cancer) and HeLa (cervical cancer) cell lines, with a clear time-dependent decrease in cell viability.

At 24 hours, cell viability decreased to 80.5%, indicating that even at early time points, allicin-loaded CuO nanoparticles have a notable impact on cell survival. By 48 hours, viability further decreased to 67.3%, demonstrating the progressive cytotoxic effect.

At 72 hours, the viability dropped to 52.7%, suggesting that prolonged exposure significantly enhances the anticancer activity of the nanoparticles. Similar trends were observed, with cell viability reducing to 76.4% at 24 hours, 62.1% at 48 hours, and 47.9% at 72 hours.

The HeLa cells showed slightly higher sensitivity to the allicin-loaded CuO nanoparticles compared to MCF-7 cells, which may be attributed to the differing cellular environments and mechanisms of response to allicin. These results suggest that allicin-loaded CuO nanoparticles are effective in inhibiting the proliferation of cancer cells, likely due to the combined effects of allicin's bioactivity and the enhanced delivery provided by the nanoparticle formulation. The nanoparticles may facilitate better cellular uptake and prolonged retention within the cells, leading to sustained cytotoxic effects. The demonstrated efficacy of allicin-loaded CuO nanoparticles against MCF-7 and HeLa cells highlights their potential for development into targeted anticancer therapies. These nanoparticles could be explored further for their ability to target other cancer types and in combination with other therapeutic agents to enhance overall treatment efficacy. Overall, the study indicates that allicin-loaded CuO nanoparticles hold significant promise as a therapeutic strategy for breast and cervical cancer, warranting further investigation and optimization for clinical applications.

CONCLUSION

The culmination of our research endeavors sheds light on the extraction, purification, and characterization of allicin from both mountain garlic (*A. montanum*) and regular garlic (*A. sativum*), along with the formulation of allicin-loaded nanoparticles. Through meticulous experimentation and optimization, we have successfully developed efficient protocols for extracting allicin from both garlic sources, achieving high yields and purity. Our comprehensive characterization studies, including TLC, FTIR, and HPLC, have confirmed the identity, purity, and chemical properties of the extracted allicin. Furthermore, our efforts in formulating allicin-loaded CuO nanoparticles using the nanoprecipitation technique have resulted in the development of stable and well-characterized nanoparticles. In addition to the technical advancements achieved in this study, our research holds broader implications for the fields of pharmaceuticals and nanomedicine.

In conclusion, our research represents a significant step forward in harnessing the therapeutic potential of allicin from garlic sources, paving the way for further exploration and development of allicin-based nanomedicines. By bridging the gap between traditional herbal medicine and modern pharmaceutical approaches, our findings contribute to the ongoing efforts to uncover nature's treasures and translate them into innovative healthcare solutions for the benefit of humanity.

REFERENCES

1. Dhakar S, Tare H, Jain SK. Exploring the Therapeutic Potential of *A. sativum*: Recent Advances and Applications. International Journal of Pharmaceutical Quality Assurance. 2023;14(4):1283-1286.
2. Alswat AA, Ahmad MB, Hussein MZ, Ibrahim NA, Saleh TA. Copper oxide nanoparticles-loaded zeolite and its characteristics and antibacterial activities. Journal of Materials Science & Technology. 2017 Aug 1;33(8):889-96.
3. Dhakar S, Tare H. Profiling Potent Medicinal Plants: *A. sativum*, Azadirachta indica, and Annona squamosa in Diabetes Management. International Journal of Drug Delivery Technology. 2024;14(1):581-588.
4. Badawi AA, El-Nabarawi MA, El-Setouhy DA, Alsammit SA. Formulation and stability testing of itraconazole crystalline nanoparticles. Aaps Pharmscitech. 2011 Sep;12:811-20.
5. Benzie IF, Szeto YT. Total antioxidant capacity of teas by the ferric reducing/antioxidant power assay. Journal of agricultural and food chemistry. 1999 Feb 15;47(2):633-6.
6. Dhakar S, Jain SK, Tare H. Exploring the Therapeutic Potential of Azadirachta indica (Neem): Recent Advances and Applications. International Journal of Pharmaceutical Quality Assurance. 2023;14(4):1211-1213.
7. Bhattacharya S, Gupta D, Sen D, Bhattacharjee C. Process intensification on the enhancement of allicin yield from *A. sativum* through ultrasound attenuated nonionic micellar extraction. Chemical engineering and processing-process intensification. 2021 Dec 1;169:108610.
8. Dhakar S, Jain SK, Tare H. Exploring the Multifaceted Potential of Annona squamosa: A Natural Treasure for Health and Wellness. International Journal of Pharmaceutical Quality Assurance. 2023;14(4):1279-1282.
9. Caballero-Florán IH, Cortés H, Borbolla-Jiménez FV, Florán-Hernández CD, Del Prado-Audelo ML, Magaña JJ, Florán B, Leyva-Gómez G. PEG 400: Trehalose Coating Enhances Curcumin-Loaded PLGA Nanoparticle Internalization in

Neuronal Cells. Pharmaceutics. 2023 May 25;15(6):1594.
10. Deng Y, Ho CT, Lan Y, Xiao J, Lu M. Bioavailability, Health Benefits, and Delivery Systems of Allicin: A Review. Journal of agricultural and food chemistry. 2023 Nov 9;71(49):19207-20.
11. Thakur P, Dhiman A, Kumar S, Suhag R. Garlic (*A. sativum* L.): A review on bio-functionality, allicin's potency and drying methodologies. South African Journal of Botany. 2024 Aug 1;171:129-46.
12. Barik S, Patra M, Gorain S, Biswas SJ. Nanotechnology in Cancer Chemoprevention: In Vivo and *In-vitro* Studies and Advancement in Biological Sciences. InModern Nanotechnology: Volume 2: Green Synthesis, Sustainable Energy and Impacts 2023 Jul 19 (pp. 203-230). Cham: Springer Nature Switzerland.
13. Ren G, Hu D, Cheng EW, Vargas-Reus MA, Reip P, Allaker RP. Characterisation of copper oxide nanoparticles for antimicrobial applications. International journal of antimicrobial agents. 2009 Jun 1;33(6):587-90.
14. Singh J, Kaur G, Rawat M. A brief review on synthesis and characterization of copper oxide nanoparticles and its applications. J. Bioelectron. Nanotechnol. 2016;1(9).
15. Naz S, Gul A, Zia M. Toxicity of copper oxide nanoparticles: a review study. IET nanobiotechnology. 2020 Feb;14(1):1-3.
16. Jadhav S, Gaikwad S, Nimse M, Rajbhoj A. Copper oxide nanoparticles: synthesis, characterization and their antibacterial activity. Journal of cluster science. 2011 Jun;22:121-9.
17. Suttee A, Singh G, Yadav N, Pratap Barnwal R, Singla N, Prabhu KS, Mishra V. A review on status of nanotechnology in pharmaceutical sciences. International Journal of Drug Delivery Technology. 2019;9:98-103.
18. Rashid AE, Ahmed ME, Hamid MK. Evaluation of antibacterial and cytotoxicity properties of zinc oxide nanoparticles synthesized by precipitation method against methicillin-resistant *Staphylococcus aureus*. International Journal of Drug Delivery Technology. 2022;12(3):985-9.
19. Abdulazeem L, Abd FG. Biosynthesis and Characterization of Gold Nanoparticles by Using Local Serratia spp. Isolate. International Journal of Pharmaceutical Quality Assurance. 2019;10(3):8-11.
20. Vishwakarma R, Tare H, Jain SK. Regulating Drug Release with Microspheres: Formulation, Mechanisms, and Challenges. International Journal of Drug Delivery Technology. 2024;14(1):487-495.
21. Al-waealy LA, Al-Dujaili AD. Histological and physiological study of the effect of silver nanoparticles and Omega-3 on Asthma of male mice induced by ovalbumin. International Journal of Pharmaceutical Quality Assurance. 2018;9(3):356-62.
22. Abid, S.M., Alaaraji, S. F. T., Khalid F. A. Alrawi. Antibacterial Activity of Copper Oxide Nanoparticles Against Methicillin Resistant *Staphylococcus aureus* (Mrsa). International Journal of Pharmaceutical Quality Assurance. 2019; 10(3): 138-141.
23. Bijwar R, Tare H. Revolutionizing Medicine: Advances in Polymeric Drug Delivery Systems. International Journal of Drug Delivery Technology. 2024;14(1):572-580
24. Jubran AS, Al-Zamely OM, Al-Ammar MH. A Study of Iron Oxide Nanoparticles Synthesis by Using Bacteria. International Journal of Pharmaceutical Quality Assurance. 2020;11(1):88-92.
25. Sonawane A, Jawale G, Devhadrao N, Bansode A, Lokhande J, Kherade D, Sathe P, Deshmukh N, Dama G, Tare H. Formulation and Development of Mucoadhesive Nasal Drug Delivery of Ropinirol HCl For Brain Targeting. International Journal of Applied Pharmaceutics. 2023;15(5):325-32.